# Modelling the effects of Omicron sub-variant BA.5 in New Zealand

Audrey Lustig, Giorgia Vattiato, Oliver Maclaren,
Leighton Watson, Samik Datta, Michael J. Plank

Submitted for internal peer review: 14 July 2022
Revised: 15 August 2022

## Summary

1. The BA.5 Omicron sub-variant is able to spread more easily than the previously dominant BA.2 sub-variant due to its immune escape characteristics. This is a key driver of the second Omicron wave in New Zealand in July/August 2022.

2. Updated modelling results that take into account new evidence for the strength of hybrid immunity suggested that the peak in new daily cases would be smaller than the peak of the first Omicron wave in March 2022.

3. Leading up to the second Omicron wave, the age distribution of cases shifted into older age groups where there is a larger susceptible population, most likely due to relatively low attack rates in the previous wave. As a result of this, the model suggested that even though daily cases were likely to peak at a level below the first Omicron wave, the peak hospital occupancy and the number of deaths could be higher than in the first Omicron wave.

4. These results suggested that public health measures such as strong uptake of booster doses, masks, widespread testing, case isolation, and ventilation would be important to reduce the load on the healthcare system through the remainder of the winter period.

# 1 Background

New Zealand's first Omicron wave was dominated by the BA.2 sub-variant which accounted for an estimated 84% of cases, with BA.1 accounting for the remaining 16%. In the week ending 29 May 2022, over 95% of sequenced new community cases were BA.2 (ESR, 2022a).

The BA.5 sub-variant was first detected in South Africa in February 2022 (Tegally et al., 2022) and is closely related to BA.2. It carries distinct mutations in the spike protein, two of which are associated with higher transmissibility and immune evasion (Cao et al., 2022; Tuekprakhon et al., 2022). BA.5 has driven waves of Covid-19 in multiple countries (UKHSA, 2022). The rise in BA.5 stems at least in part from its ability to infect people who were immune to earlier variants, but so far there is no indication the variant causes more severe disease.

BA.5 was first detected in the New Zealand community in April 2022 and cases have been appearing consistently since May. It quickly rose to 32% of sequenced community cases by the beginning of July and became the dominant variant in early July 2022 (ESR, 2022a).

Here we show results from a mathematical model that was used to estimate the potential impact of the BA.5 sub-variant in New Zealand under various scenarios. The model includes the effects of vaccine-derived and infection-derived immunity, waning, reinfection and immune escape of the BA.5 sub-variant.

# 2 Results

Results were fitted to data available as at 7 July 2022 on new daily cases, hospitalisations and deaths, and the incidence of infections in a cohort of routinely tested border workers. Note that hospitalisations exclude those who are not being treated primarily for Covid-19 and deaths exclude those that are classified as not related to Covid-19 by the Ministry of Health. To allow for reporting lags, the most recent 40 days of admissions data (admissions after 28 May 2022) and 10 days of deaths data (deaths after 27 June 2022) were excluded. In addition, the model was updated on 15 July 2022 in light of new research on the effectiveness of immunity from prior infection with Omicron (Altarawneh et al., 2022; Hansen et al., 2022; Malato et al., 2022) (see Methods) and new Ministry of Health data on the number of possible reinfections occurring in New Zealand (Ministry of Health, 2022).

Figure 1 shows model results for the baseline scenario (in which BA.5 has a growth rate of 0.09 per day relative to BA.2) and assuming that contact rates and government policy do not change in response to the wave. The growth advantage of BA.5 was estimated from data on sequenced community cases up to 21 June 2022 (ESR, 2022b) - see Supplementary Figure 1. Scenarios where BA.5 has a smaller/larger growth advantage are shown in Figures 2 and 3 respectively.

Comparing to subsequently reported data up to 8 August 2022, the peak in new daily cases was earlier and slightly lower than the median model estimate in Fig. 1b, although the height of the peak was within the interquartile range of model simulations. Due to reporting lags, it

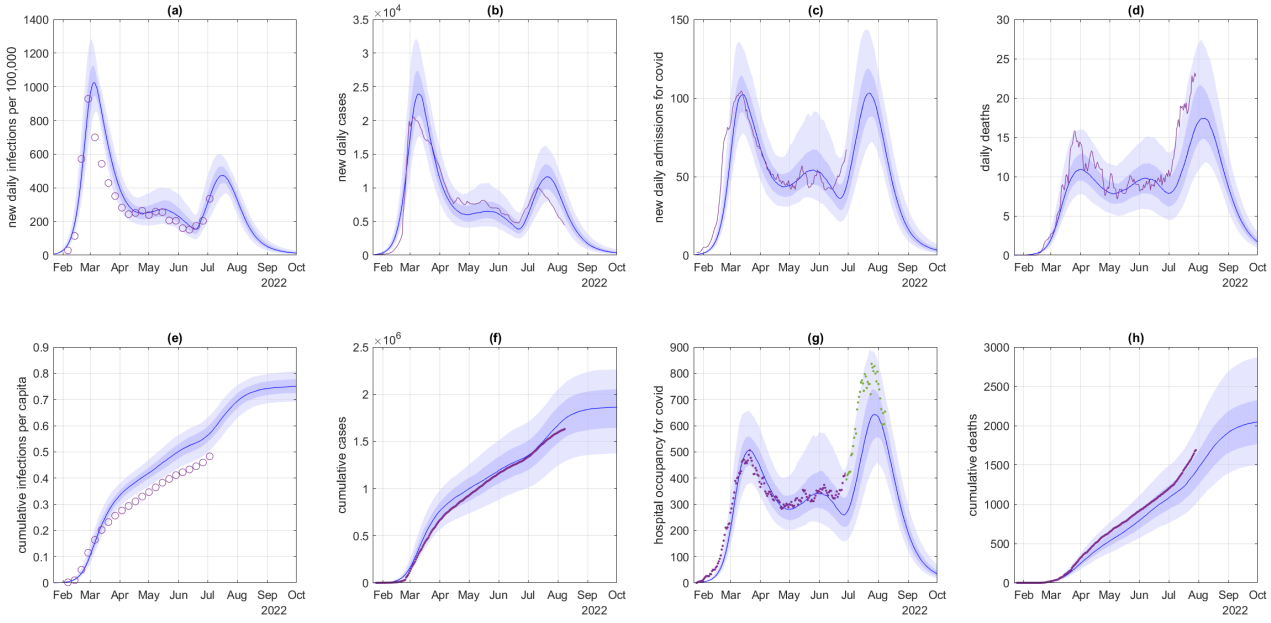


Figure 1: Results for the baseline scenario with no reduction in transmission: (a) new daily infections per 100,000 people, (b) new daily reported cases, (c) new daily hospital admissions, (d) daily deaths, (e) cumulative infections, (f) cumulative cases, (g) number of hospital beds occupied with Covid-19 patients, (h) cumulative deaths. Blue curves show the median of 500 model simulations and shaded bands show the 5th, 25th, 75th and 95th percentiles. Purple curves/points show data as at 9 August 2022; data shown in (b)–(d) is a 7-day rolling average. Note these graphs exclude hospital patients who are not being treated primarily for Covid-19 and deaths that are classified as not related to Covid-19. Data for new daily infections per 100,000 show the rate of cases detected in a routinely tested cohort of approximately 20,000 border workers. Reported cases are lower than total infections due to under-reporting. The most recent 10 days of deaths data and 40 days of admissions data are excluded due to reporting lags. The number of patients being treated for Covid-19 shown in (g) is calculated from individual-level Ministry of Health data up to 29 June 2022 on date of admission and number of days receiving hospital treatment for Covid-19 (purple points); after 29 June 2022 individual-level data is incomplete so the data shows the total national hospitalisations reported by the Ministry of Health in 1pm updates (green points).

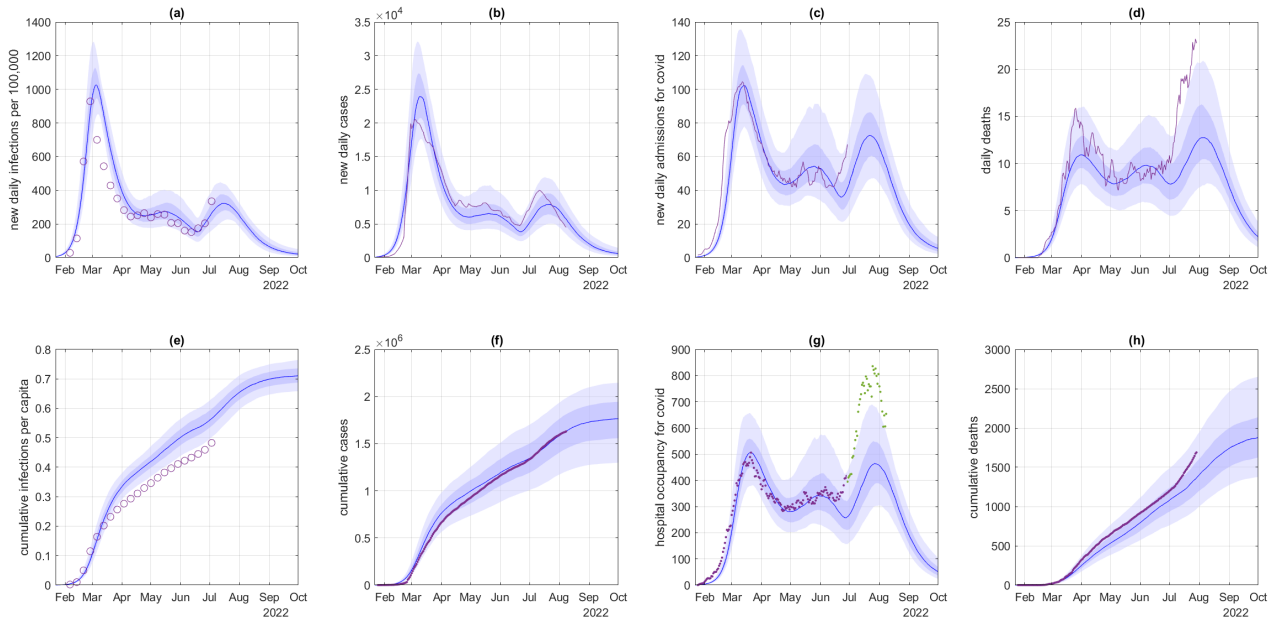


Figure 2: As for Figure 1 but with a smaller growth advantage for BA.5 relative to BA.2 (0.07 day$^{-1}$ instead of 0.09 day$^{-1}$).

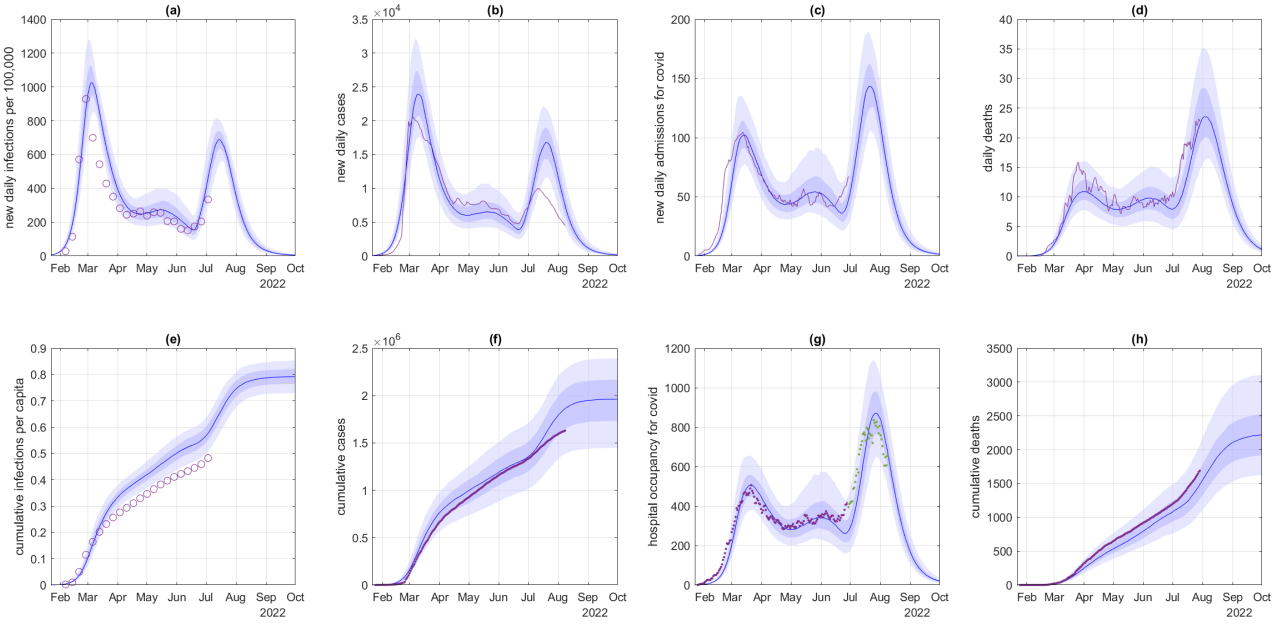


Figure 3: As for Figure 1 but with a larger growth advantage for BA.5 relative to BA.2 (0.12 day$^{-1}$ instead of 0.09 day$^{-1}$).

is too early to definitively compare peak hospitalisations and deaths to the model. Provisional estimates for hospitalisations based on the total number of Covid-19 cases in hospital reported by the Ministry of Health in 1pm updates (Fig. 1g, green points) peaked above the median model estimate but within the 90% range. The number of daily deaths attributed to Covid-19 (Fig. 1d) is also tracking above the median model estimate but within the 90% range. These data likely include some hospitalisations and deaths that are unrelated to Covid-19, and are subject to change as data on primary reason for hospitalisation or cause of death become available. However, it is likely that the number of people receiving hospital treatment for Covid-19 and the number of daily deaths attributed to Covid-19 both peaked at significantly higher levels than in March 2022. The high number of cases in over-70-year-olds (see Supplementary Figure 2) is likely a key contributor to the high number of hospitalisations and deaths relative to the number of cases.

## Model limitations

The model is a simplified representation of a complex and rapidly evolving epidemiological situation. It attempts to capture the most important mechanisms affecting epidemic dynamics, but has significant limitations. The results should be treated as an indication of likely outcomes under a range of different scenarios and should not be relied on as accurate predictions. Major sources of uncertainty include:

- New Zealand lacks representative sampling of SARS-CoV-2 prevalence and reported cases are likely to be a significant underestimate of total infections. This means that the total number people infected with Omicron to date is unknown and therefore the extent of infection-derived immunity in the population is uncertain.
- Unlike previous waves, immunity is now the single biggest factor affecting transmission dynamics. The immune landscape in New Zealand has become more complex, with various combinations of immunity derived from vaccination and prior infection at different time points. The model necessarily makes simplifying assumptions about the nature of the immunity landscape and it is possible that results are sensitive to these assumptions.
- The extent, if any, of behavioural change in response to the BA.5 wave was difficult to predict. Although behavioural change is known to have had a significant effect on previous waves in New Zealand and internationally, it cannot be assumed that the response would be comparable for the current wave.
- Estimates for the level of immune escape of BA.5 are uncertain and this is a key factor determining the size of the wave. We estimated the growth advantage of BA.5 relative to BA.2 from data on sequenced community cases reported up to 21 June 2022. Although this gave an estimate that is consistent with international estimates (UKHSA, 2022), it should be remembered that sequenced cases are not necessarily representative of all cases and there is still a range of possible values for the BA.5 growth rate. We attempted to investigate this uncertainty with the additional scenarios shown in Figures 2 and 3.

- The effect of immune escape and reinfection on the risk of severe disease and death is also uncertain and this will affect the projected case hospitalisation ratio and case fatality ratio. Here, due to a lack of evidence to the contrary, we assumed that there is no change in disease severity for BA.5 compared to BA.2.
- The model assumes that mixing within and between age groups can be reasonably approximated by an age-structured contact matrix. It is likely that population heterogeneity not accounted for in the model has a significant effect on the point at which new infections peak and start to decline (the herd immunity threshold).
- The size and timing of peaks are inherently uncertain because they are sensitive to variables and parameters that are not precisely known including those mentioned above.
- We have only modelled the aggregate impacts of the BA.5 wave at the national level. These results will mask significant regional and demographic variation. Some groups are likely to be disproportionately affected such as those working in public-facing roles and insecure employment, people in overcrowded or substandard housing, Māori and Pacific people (Steyn et al., 2021), and people without good access to healthcare, testing, masks and vaccines.

# 3 Methods

The susceptible population is divided into $n_A$ age groups and $n_S$ susceptible compartments per age group, denoted $S_{ik}$ for $i = 1, \ldots, n_A$ and $k = 1, \ldots, n_S$. The susceptible states represents different levels of vaccine-derived and infection-derived immunity (Figure 4). Each state $k$ is associated with a set of immunity parameters $e_{Ok}$ representing immunity against different outcomes $O$ (see section 3.4).

For each susceptible compartment, there are associated compartments for people who are: exposed but not yet infectious ($E$); infectious and with clinical symptoms ($I$); infectious and subclinical ($A$); recovered and temporarily immune ($R$). Note that subclinical refers to people who never develop symptoms. For simplicity we do not distinguish between the pre-symptomatic and symptomatic stages of the infectious period for clinical individuals, although it would be straightforward to do this, for example to model symptom-based interventions.

The model structure is similar to that of the stochastic individual-based model of Vattiato et al. (2022) but is generalised to include waning of infection-derived immunity and the effects of fourth and potentially subsequent doses of the vaccine. Using a deterministic model ignores stochastic fluctuations in daily infection rates, although this is likely to have a relatively small effect on epidemic dynamics during periods of relatively high prevalence. In addition, high levels of prior infection mean that transmission is primarily controlled by immunity, which creates negative feedback on stochastic deviations from a mean-field model. The waning model is similar conceptually to Keeling et al. (2021) but the inclusion of a series of post-recovery susceptible compartments means the model is not restricted to exponential waning curves and can capture differing dynamics of immunity against infection and immunity against severe disease.

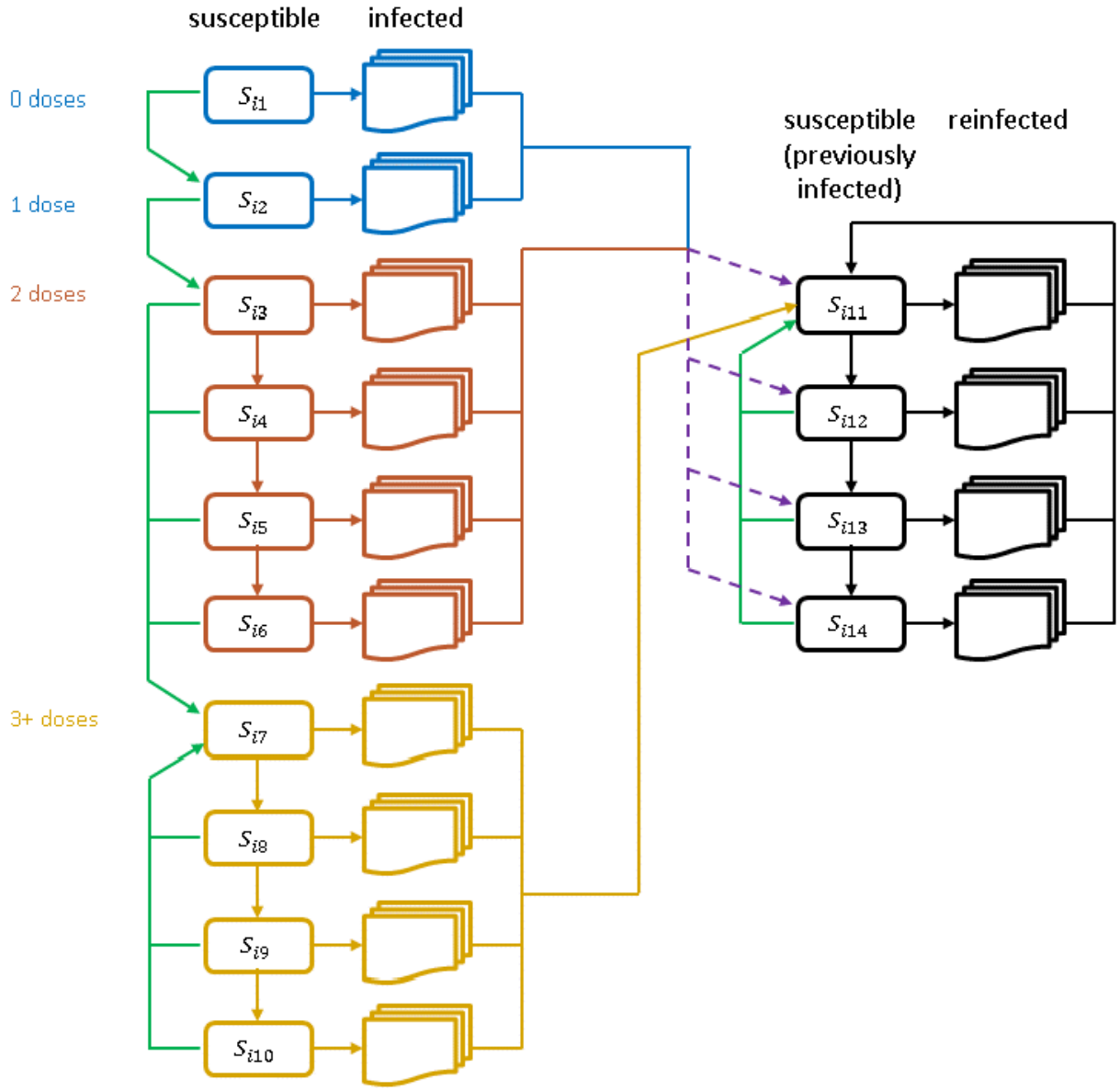


Figure 4: Schematic diagram of the model structure showing the 14 susceptible compartments for age group $i$, indexed as compartments $S_{ik}$ for $k = 1, \ldots, 14$. Vertical downward arrows represent transition to a susceptible compartment with lower immunity as a result of waning immunity. Green arrows represent transition to a susceptible compartment with higher immunity as a result of vaccination. Horizontal arrows represent infection, which initiates transition through a series of disease states ending in recovery. Following recovery from first infection, individuals who have had at least three vaccine doses (yellow) transition to the highest immunity post-infection compartment $S_{i,11}$; individuals who have had less than three vaccine doses (blue and red) transition to a mixture of compartments $S_{i,11}$ to $S_{i,14}$ (dashed purple arrows), representing lower post-infection immunity for these groups. Following recovery from a second or subsequent infection (black), all individuals transition to $S_{i,11}$ regardless of vaccination status.

## 3.1 Transmission dynamics

The transmission dynamics are governed by a set of ordinary differential equations for these compartments:

$$\frac{dS_{ik}}{dt} = -\lambda_i(1-e_{I,k})S_{ik} + W_{ik} + G_{ik} \quad (1)$$

$$\frac{dE_{ik}}{dt} = \lambda_i(1-e_{I,k})S_{ik} - 1/t_E E_{ik} \quad (2)$$

$$\frac{dI_{ik}}{dt} = 1/t_E p_{\text{clin},i}(1-e_{S,k})E_{ik} - 1/t_I I_{ik} \quad (3)$$

$$\frac{dA_{ik}}{dt} = 1/t_E\left(1-p_{\text{clin},i}(1-e_{S,k})\right)E_{ik} - 1/t_I A_{ik} \quad (4)$$

$$\frac{dR_{ik}}{dt} = 1/t_I(I_{ik}+A_{ik}) - r_w\hat{r}R_{ik}, \quad (5)$$

where $t_E$ and $t_I$ are the latent and infectious periods, respectively, $p_{\text{clin},i}$ is the probability of testing for a clinical infection, $r_w$ is the waning rate, and $\hat{r}$ is the relative rate of moving from recovered ($R$) to susceptible ($S$). Parameter values are listed in Tables 1 and 2.

The $W_{ik}$ and $G_{ik}$ terms represent waning and vaccination dynamics (see Sec. 3.2). The force of infection $\lambda_i$ acting on age group $i$ is:

$$\lambda_i = \frac{UR_{EI}(t)u_i}{t_I N_i}\sum_{j=1}^{n_A} M_{ji}\left[\sum_{k=1}^{n_S}(1-e_{T,k})(I_{jk}+\tau A_{jk}) + t_I n_{\text{seed},j}(t)\right] \quad (6)$$

where $R_{EI}(t)$ is the time-varying reproduction number excluding effects of immunity, $N$ is the total population size in each age group, $n_{\text{seed},j}(t)$ is the number of daily seed infections in age group $j$ at time $t$, $\tau$ is the relative infectiousness of subclinical individuals, $u_i$ is the susceptibility of age group $i$ relative to the 60-64 year age group, and $M_{ji}$ is the average number of daily contacts in age group $i$ by someone in age group $j$. The normalising constant $U$ is set to be

$$U = \rho\left[\left(p_{\text{clin},j} + \tau(1-p_{\text{clin},j})\right)u_i M_{ji}\right]^{-1}$$

where $\rho[.]$ denotes dominant eigenvalue. This normalisation ensures that the reproduction number at time $t$ would be $R_{EI}(t)$ in a fully susceptible population. The contact matrix $M$ is based on the results of Prem et al. (2017), adjusted for the New Zealand population by Vattiato et al. (2022).

Because $R_{EI}(t)$ represents the value the reproduction number would take if there was no immunity in the population, it is unaffected by vaccination, infection and waning dynamics. It therefore provides a way to model time-dependence in contact rates, for example as a result of behavioural change or policy response.

## 3.2 Vaccination and waning

As indicated above, the $G_{ik}$ term in Eq. (1) represents transitions between susceptible compartments that occur as a result of vaccination (green arrows in Figure 4). For the purposes of

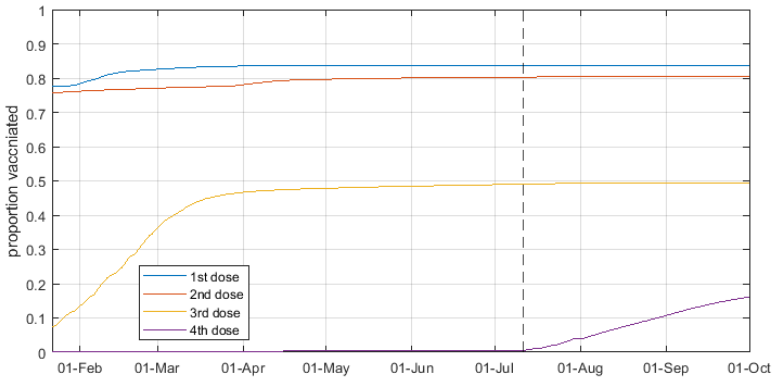


Figure 5: Cumulative number of 1st, 2nd, 3rd and 4th doses of the vaccine relative to New Zealand's population size, based on actual doses administered up to 11 July 2022 (dashed vertical line) and Ministry of Health projections of future uptake of 4th doses after 11 July 2022.

calculating this, we define five groups of susceptible compartments $S^g$:

$$\text{0 doses and not previously infected:} \quad S^g_{i0} = S_{i1} \tag{7}$$

$$\text{1 dose and not previously infected:} \quad S^g_{i1} = S_{i2} \tag{8}$$

$$\text{2 doses and not previously infected:} \quad S^g_{i2} = \sum_{k=3}^{6} S_{ik} \tag{9}$$

$$\geq \text{3 doses and not previously infected:} \quad S^g_{i3} = \sum_{k=7}^{10} S_{ik} \tag{10}$$

$$\text{previously infected:} \quad S^g_{ip} = \sum_{k=11}^{14} S_{ik} \tag{11}$$

We assumed that all vaccine doses are given to people who are in a susceptible compartment (which is reasonable given the recommendation to wait at least 3 months after testing positive before getting vaccinated).

The total number of people $V_{id}(t)$ in each age group who have received at least $d$ doses of the vaccine at time $t$ is:

$$\frac{dV_{id}}{dt} = v_{id}(t) \tag{12}$$

where $v_{id}(t)$ is the number of $d^{\text{th}}$ doses per day given to people in age group $i$ at time $t$, plus estimated future uptake of fourth doses according to Ministry of Health projections (see Figure 5).

We assumed that the $v_{id}$ $d^{\text{th}}$ doses ($d = 1, 2, 3$) given to people in age group $i$ at time $t$ are split pro rata between people who have not been previously infected and people who have. This implies that the daily proportion of those not previously infected in age group $i$ receiving their $d^{\text{th}}$ dose at time $t$ is

$$p^u_{i,d} = \frac{v_{i,d}}{V_{i,d-1} - V_{i,d}} \tag{13}$$

noting that $V_{i,0} = N_i$, i.e. the total population size in age group $i$. This accounts for $p^u_{i,d} S^g_{i,d-1}$ of the $v_{i,d}$ doses. The remainder of these doses, $v_{i,d} - p^u_{i,d} S^g_{i,d-1}$, are given to previously infected people. This implies that the daily proportion of those previously infected in age group $i$ receiving their $d^{\text{th}}$ dose at time $t$ is

$$p^p_{i,d} = v_{i,d} \frac{V_{i,d-1} - V_{i,d} - S^g_{i,d-1}}{(V_{i,d-1} - V_{i,d}) S^g_{i,p}} \tag{14}$$

The corresponding equations for 4th or subsequent doses are

$$p^u_{i,4+} = \frac{v_{i,4+}}{V_{i,3}} \tag{15}$$

$$p^p_{i,4+} = v_{i,4+} \frac{V_{i,3} - S^g_{i,3}}{V_{i,3} S^g_{i,p}} \tag{16}$$

We may then write the proportion of compartment $S_{ik}$ receiving a vaccine dose per day as:

$$P_{i,k} = \begin{cases} p^u_{i,1}, & \text{if } k = 1 \\ p^u_{i,2}, & \text{if } k = 2 \\ p^u_{i,3}, & \text{if } 3 \leq k \leq 6 \\ p^u_{i,4+}, & \text{if } 7 \leq k \leq 10 \\ \sum_{d=1}^{4+} p^p_{i,d}, & \text{if } 11 \leq k \leq 14 \end{cases} \tag{17}$$

We assume that receiving a vaccine dose following prior infection has the effect of moving people back to the first post-infection compartment ($S_{i,11}$) and that receiving a 4th dose without any prior infection has the effect of moving people back to the first 3-dose compartment ($S_{i,7}$).

The term $G_{ik}$ appearing in Eq. (1) is now defined as:

$$G_{ik} = \sum_{l=1}^{n_S} P_{il} S_{il} Q^V_{lk} \tag{18}$$

where $Q^V_{lk}$ is the flux into susceptible compartment $k$ from susceptible compartment $l$ as a result of vaccine doses given to people in susceptible compartment $l$, such that the row sums of the matrix $Q^V$ are all 0.

The term $W_{ik}$ in Eq. (1) represents transitions between susceptible compartments, and transitions from recovered to susceptible compartments, that occur as a result of waning and is defined as:

$$W_{ik} = r_w \left( \sum_{l=1}^{n_S} S_{il} Q^S_{lk} + \hat{r} \sum_{l=1}^{n_S} R_{il} Q^R_{lk} \right) \tag{19}$$

where $Q^S_{lk}$ is the flux into susceptible compartment $k$ from susceptible compartment $l$ (with $Q^S_{kk} \leq 0$ representing the flux out of compartment $k$) such that the row sums of the matrix $Q^S$ are all 0; and $Q^R_{kl} \geq 0$ is the flux into susceptible compartment $k$ from recovered compartment $l$ such that the row sums of $Q^R$ are all 1.

## 3.3 Clinical pathways

The process of testing and progress to different clinical endpoints (hospital admission, hospital discharge, and death) can be modelled downstream of the transmission dynamics. We model the number of newly infectious people in each age group who will eventually become a confirmed case ($C$), be hospitalised ($H$), and die ($F$) via the differential equations.

$$\frac{dC_{i1}}{dt} = 1/t_E \sum_{k=1}^{n_S} \left( p_{\text{test,clin}} p_{\text{clin},i} \frac{1-e_{S,k}}{1-e_{I,k}} + p_{\text{test,sub}} \left( 1 - p_{\text{clin},i} \frac{1-e_{S,k}}{1-e_{I,k}} \right) \right) E_{ik} - \alpha_1 C_{i1} \quad (20)$$

$$\frac{dH_{i1}}{dt} = 1/t_E IHR_i \sum_{k=1}^{n_S} \frac{1-e_{H,k}}{1-e_{I,k}} E_{ik} - \alpha_1 H_{i1} \quad (21)$$

$$\frac{dF_{i1}}{dt} = 1/t_E IFR_i \sum_{k=1}^{n_S} \frac{1-e_{F,k}}{1-e_{I,k}} E_{ik} - \alpha_1 F_{i1} \quad (22)$$

$$(23)$$

The time lag from onset of infectiousness to each endpoint is modelled via transition through a series of compartments:

$$\begin{array}{lll} \frac{dC_{i,2}}{dt} = \alpha_1 C_{i1} - \alpha_2 C_{i2}, & \frac{dH_{i,2}}{dt} = \alpha_1 H_{i1} - \alpha_2 H_{i2}, & \frac{dF_{i,2}}{dt} = \alpha_1 F_{i1} - \alpha_2 F_{i2}, \\ \frac{dC_{i,3}}{dt} = \alpha_2 C_{i2}, & \frac{dH_{i,3}}{dt} = \alpha_2 H_{i2} - \alpha_3 H_{i3}, & \frac{dF_{i,3}}{dt} = \alpha_2 F_{i2} - \alpha_3 F_{i3}, \\ & \frac{dH_{i,4}}{dt} = \alpha_3 H_{i3} - \alpha_{4,i} H_{i4}, & \frac{dF_{i,4}}{dt} = \alpha_3 F_{i3} - \alpha'_4 F_{i4}, \\ & \frac{dH_{i,5}}{dt} = \alpha_{4,i} H_{i4}, & \frac{dF_{i,5}}{dt} = \alpha'_4 F_{i4} - \alpha_5 F_{i5}, \\ & & \frac{dF_{i,6}}{dt} = \alpha_5 F_{i5}. \end{array} \quad (24)$$

where $\alpha_k$ are a set of rate constants determining the time lags. We set $\alpha_1 = \alpha_2 = 2/t_T$ where $t_T$ is the mean time from onset of infectiousness to return of a positive test result. The mean time from positive test result to hospital admission is $t_H = \alpha_3^{-1}$, and the mean length of hospital stay for non-fatal cases in age group $i$ is $t_{LOS,i} = \alpha_{4,i}^{-1}$. We set $\alpha'_4 = \alpha_5 = 2/t_F$ where $t_F$ is the mean time from hospital admission to death.

The compartment $C_{i3}$ represents the observed cumulative number of cases, $H_{i4}$ the number of cases currently in hospital, $H_{i5}$ the cumulative number of hospital discharges and $F_{i6}$ the cumulative number of fatalities in age group $i$ at time $t$. The other $C$, $H$ and $F$ variables above represent latent (unobservable) states.

## 3.4 Immunity model

The immunity parameters $e_{Ik}$, $e_{Sk}$, $e_{Tk}$, $e_{Hk}$ and $e_{Fk}$ respectively represent the immunity against infection, symptomatic disease, transmission, hospitalisation and death for people in susceptible compartment $k$. A value $e = 0$ corresponds to no immunity and $e = 1$ corresponds to complete immunity. In total there are up to 70 immunity parameters in the model (14 susceptible compartments times 5 endpoints). To provide a parsimonious parameterisation, we use a

| Parameter | Value |
|---|---|
| Initial log antibody titre: | |
| - 2 doses | $n_{2d,0} = -1.61$ |
| - 3 doses | $n_{3d,0} = -0.92$ |
| - prior infection with 0/1 doses | $n_{p,0} = 1.39$ |
| - prior infection with 2 doses | $n_{p2d,0} = 2.71$ |
| - prior infection with 3 doses | $n_{p3d,0} = 3.56$ |
| Log antibody titre providing 50% immunity: | |
| - against infection | $n_{\text{inf},50} = -1.61$ |
| - against hospitalisation | $n_{\text{hosp},50} = -3.51$ |
| - against death | $n_{\text{death},50} = -3.51$ |
| Waning rate | $r_w \sim U(0.0027, 0.0063)$ day$^{-1}$ |
| Relative rate of moving from $R$ to $S$ | $\hat{r} = 1.85$ |
| Drop in log titre in subsequent compartment | $n_{\text{drop}} = 2.30$ |
| Slope of logistic function | $\kappa = 1.28$ |
| Minimum long-term immunity to hospitalisation and death | $e_{\text{sev,min}} = 0.5$ |

Table 1: Parameters for the immunity submodel. All log titres are given as natural logarithms and represent neutralisation of BA.2. The drop in neutralising titre for BA.5 relative to BA.2 is described in Sec. 3.6.

conceptual model where a given source of immunity (vaccination and/or prior infection) is associated with a neutralising antibody titre that decays over time (Khoury et al., 2021; Cromer et al., 2022b). The antibody titre is assumed to be a correlate of protection, and a given titre is generally more protective against more serious clinical endpoints, in line with the findings of Cromer et al. (2022a). This framework enables laboratory data from virus neutralisation experiments to be combined with population-level data to produce estimates of time-varying immunity from different sources, to different endpoints, resulting from infection with different variants of SARS-CoV-2 (Golding and Lydeamore, 2022).

Using the estimates of Golding and Lydeamore (2022), we determine the mean initial log antibody titre $n_{i,0}$ associated with each source of immunity $i$ in our model (2 or 3 vaccine doses with or without prior infection). To represent decay in antibody titre over time, we assume that the log antibody titre decreases by a fixed amount for each successive susceptible compartment in the same category (i.e. through compartments $k = 3, \ldots, 6$, $k = 7, \ldots, 10$ and $k = 11, \ldots, 14$). We then map the log antibody titre $n_k$ for compartment $k$ to immunity $e_{Ok}$ against outcome $O$ via a logistic function with an outcome-specific midpoint parameter $n_{O,50}$ (Khoury et al., 2021):

$$e_{Ok} = \frac{1}{1 + e^{-\kappa(n_k - n_{O,50})}} \tag{25}$$

This framework means the immunity model can be parameterised with one parameter $n_{i,0}$ for each source of immunity $i$, one parameter for each outcome $O$ and two additional independent parameters: the logistic slope $\kappa$; and the transition rate $r_w$ between successive susceptible compartments, which represents the speed of waning (see Table 1).

We assume immunity for people who are (transiently) in the one-dose compartment is negligible. Hence $e_{O1} = e_{O2} = 0$ for all outcomes $O$. We set the log antibody titre for susceptible compart-

ments $k = 3$ and $k = 7$ equal to the estimates of Golding and Lydeamore (2022) for the initial log neutralising titre for 2 doses $n_{2d,0}$ and 3 doses $n_{3d,0}$ respectively of the Pfizer/BioNTech BNT162b2 vaccine against Omicron (Table 1).

For the post-infection susceptible states, we do not have separate susceptible compartments for people with different vaccination status. Instead, the log titre for first post-infection susceptible compartment $k = 11$ represents the log titre for prior infection plus 3 doses $n_{p3d,0}$. Following recovery from a first infection, people with 3 doses of the vaccine (i.e. those in recovered compartments $k = 7, \ldots, 10$) all move initially to susceptible compartment $k = 11$. This is encoded by the matrix $Q^R$ in Eq. (19): $Q^R_{k,11} = 1$ for $k = 7, \ldots 10$.

To model lower levels of post-infection immunity for people who have had fewer than 3 doses of the vaccine, following recovery from a first infection, a fixed proportion of these people move to the lower-immunity compartments $k = 12, 13, 14$. To determine what this proportion should be, we first note that, absent any subsequent immunising events, the proportion $q_k(t)$ of a cohort of individuals entering susceptible compartment $k = 11$ at time $t = 0$ that is in compartment $k$ at time $t$ satisfies

$$\dot{q}_k = \begin{cases} -r_w q_k, & k = 11 \\ r_w(q_{k-1} - q_k), & k = 12, 13 \\ r_w q_{k-1}, & k = 14 \end{cases} \tag{26}$$

where $q_{11}(0) = 1$ and $q_k(0) = 0$ for $k = 11, 12, 13$. The average log antibody titre of the cohort at time $t$ is $\bar{n}(t) = \sum_k n_k q_k(t)$.

For people with 2 doses of the vaccine prior to first infection (i.e. people in recovered compartments $k = 3, \ldots, 6$), we set $Q^R_{kl} = q_l(t^*)$ where $t^*$ is such that $\bar{n}(t^*) - \bar{n}(0) = n_{p2d,0} - n_{p3d,0}$, the estimated difference in initial log titre between prior infection plus 2 doses and prior infection plus 3 doses according to Golding and Lydeamore (2022). Similarly, for people with 0 or 1 doses prior to first infection (i.e. people in recovered compartments $k = 1, 2$), we set $Q^R_{kl} = q_l(t^*)$ where $t^*$ is such that $\bar{n}(t^*) - \bar{n}(0) = n_{p,0} - n_{p3d,0}$. Following recovery from a second or subsequent infection, everyone moves initially to susceptible compartment $k = 11$ regardless of vaccination status: $Q^R_{k,11} = 1$ for $k = 11, \ldots, 14$.

For simplicity, we set $e_{Tk} = 0$ and $e_{Sk} = e_{Ik}$, i.e. immunity reduces the risk of infection but, conditional on infection, does not change the likelihood of symptomatic disease or transmission. We also assume that immunity against hospitalisation and death never wane below $e_{\text{sev,min}} = 0.5$. This models a more durable component of the immune response, for example cellular immunity as opposed to neutralising antibodies, that maintains immunity against severe disease at some minimum long-term level. For the initial log titre following infection, we use higher values than those estimated by Golding and Lydeamore (2022), based on partly on recent epidemiological studies suggesting that prior infection with BA.1/BA.2 provides relatively strong immunity against reinfection at least for a few months (Altarawneh et al., 2022; Hansen et al., 2022; Malato et al., 2022). Average immunity from different sources against infection and against severe disease are shown in Figure 6.

## 3.5 Population dynamics

The dynamics of birth, death and ageing can be incorporated into the model via additional terms in Eqs. (1)–(12) of the form:

$$\frac{dX_{1,k}}{dt} = b - r_a X_{1,k} - \mu_1 X_{1,k} \quad (27)$$

$$\frac{dX_{i,k}}{dt} = r_a(X_{i-1,k} - X_{i,k}) - \mu_i X_{i,k} \quad (28)$$

$$\frac{dX_{n_A,k}}{dt} = r_a X_{n_A-1,k} - \mu_{n_A} X_{n_A,k} \quad (29)$$

where $b$ is the birth rate per unit time, $r_a$ is ageing rate per unit time (equal to the reciprocal of the size of the age bands, in this case 5 years) and $\mu_i$ is the per capita death rate per unit time in age group $i$. Here $X$ may be any one of the infection states ($S$, $E$, $I$, $A$, $R$) or $V$. For simplicity we assume that the the aggregate population death rate is independent of the transmission dynamics.

The total number of annual births and the annual death rate in 5-year age bands up to age 75 were taken from StatsNZ data for 2019 (StatsNZ, 2022). The annual death rate for the over-75-years age group was set to give a similar equilibrium age distribution to the StatsNZ 2022 estimated resident population (StatsNZ, 2022).

## 3.6 Variant model

To model the effect of a new variant, we use a simplified approach that captures potential changes in intrinsic transmissibility and/or immune escape. This does not encompass the full dynamics of two or more variants spreading simultaneously but captures the key effects by changing relevant model parameters around a specified time point $t_{VOC}$ when the new variant becomes dominant. For simplicity, we assume that all infections prior to $t_{VOC}$ are the resident variant (BA.2) and all infections after $t_{VOC}$ are the new variant (BA.5).

A variant that has different intrinsic transmissibility can be modelled by a change in the parameter $R_{EI}(t)$ at $t = t_{VOC}$. A variant that evades immunity can be modelled by reducing the initial antibody titre levels $e_{2d,0}$ and $e_{3d,0}$ for vaccinated but not previously infected states at $t = t_{VOC}$ (Khoury et al., 2021). This is equivalent to a reduction in vaccine effectiveness. We assume that BA.5 has the same intrinsic transmissibility as BA.2, but there is a 2.5-fold drop in antibody titre against BA.5 relative to BA.2, which is consistent with lab studies on neutralisation (Khan et al., 2022; Hachmann et al., 2022).

Reducing the initial antibody titre for previously infected states ($k = 11, \ldots, 14$) would result in a permanent reduction in infected-induced immunity, including against future reinfection with the same variant. To avoid this, we instead model reduction in infection-derived antibody titre to the new variant by moving individuals in the previously infected states ($S_{11}$, $S_{12}$ or $S_{13}$) at $t = t_{VOC}$ to a lower immunity state ($S_{12}$, $S_{13}$ or $S_{14}$). This means that there is a reduction in average titre applied to people infected before $t = t_{VOC}$ (assumed to be infection

| Parameter | Value |
|---|---|
| *Epidemiological parameters* | |
| Latent period | $t_E = 1$ day |
| Infectious period | $t_I = 2.3$ days |
| Mean time from onset of infectiousness to positive test result | $t_T = 4$ days |
| Mean time from test result to hospital admission | $t_H = 1$ days |
| Mean time from admission to death | $t_F = 14$ days |
| Relative infectiousness of subclinical individuals | $\tau = 0.5$ |
| Probability of testing (clinical) | $p_{\text{test,clin}} \sim U(0.35, 0.75)$ |
| Probability of testing (sublinical) | $p_{\text{test,sub}} = 0.4 p_{\text{test,clin}}$ |
| *Date-specific parameters* | |
| Date of seeding with infectious cases | 19 Jan 2022 $+U(-3, 3)$ |
| Number of seed cases in age group $i$ | $0.0001 N_i$ |
| $R_{EI}(t)$ in period 1 | $R_{EI,1} \sim U(2.0, 2.4)$ |
| $R_{EI}(t)$ in period 2 | $R_{EI,2} \sim U(2.9, 4.9)$ |
| End of period 1 | 10 Mar 2022 $+U(-5, 5)$ |
| Period 1 – period 2 ramp window | $U(35, 75)$ days |
| Relaxation of contact matrix | $\alpha_M \sim U(0, 0.8)$ |
| Contact matrix ramp window | $U(50, 90)$ days |
| *Variant model* | |
| BA.5 immune escape [low,baseline,high] | $r_{VOC} = [0.19, 0.39, 0.59]$ |
| BA.5 change in vaccine-derived log antibody titre relative to BA.2 | $\Delta n_{0,VOC} = -0.92$ |
| BA.5 dominance date | $t_{VOC} = 20$ Jun 2022 |
| Variant transition window | $\sigma_{VOC} = 2$ days |

Table 2: Model parameter values and prior distributions.

| Age (yrs) | Popn $N_i(0)$ | $u_i$ | $p_{\text{clin},i}$ | $IHR_i$ per 1000 | $IFR_i$ per 1000 | $t_{LOS,i}$ (days) | $\mu_i$ (per 1000 per yr) |
|---|---|---|---|---|---|---|---|
| 0-4 | 305055 | 0.46 | 54% | 0.94 | 0.0034 | 2.0 | 1.07 |
| 5-9 | 327520 | 0.46 | 55% | 0.94 | 0.0034 | 2.0 | 0.08 |
| 10-14 | 336975 | 0.45 | 58% | 0.40 | 0.0034 | 2.0 | 0.17 |
| 15-19 | 316980 | 0.56 | 60% | 0.60 | 0.0062 | 2.0 | 0.41 |
| 20-24 | 329695 | 0.79 | 62% | 0.87 | 0.012 | 2.0 | 0.60 |
| 25-29 | 370120 | 0.93 | 64% | 1.25 | 0.024 | 2.0 | 0.56 |
| 30-34 | 379010 | 0.97 | 66% | 1.84 | 0.048 | 2.7 | 0.73 |
| 35-39 | 340755 | 0.98 | 68% | 2.69 | 0.091 | 3.3 | 0.83 |
| 40-44 | 312245 | 0.94 | 70% | 3.81 | 0.180 | 4.0 | 1.21 |
| 45-49 | 325050 | 0.93 | 71% | 5.61 | 0.360 | 4.7 | 1.95 |
| 50-54 | 333210 | 0.94 | 73% | 8.32 | 0.697 | 5.4 | 3.07 |
| 55-59 | 325780 | 0.97 | 74% | 11.7 | 1.35 | 6.0 | 4.45 |
| 60-64 | 298820 | 1.00 | 76% | 16.9 | 2.65 | 6.7 | 6.49 |
| 65-69 | 254865 | 0.98 | 77% | 23.8 | 5.08 | 7.4 | 10.27 |
| 70-74 | 220245 | 0.90 | 78% | 33.3 | 9.74 | 8.0 | 16.69 |
| 75+ | 346280 | 0.86 | 80% | 59.7 | 54.7 | 8.7 | 136.0 |

Table 3: Age-dependent model parameters: 'Popn' is the initial population size in each age group; $u_i$ is the susceptibility of age group $i$ relative to the 60-64 year age group; $p_{clin,i}$, $IHR_i$ and $IFR_i$ are respectively the proportion of infections causing clinical disease, hospitalisation and death respectively for individuals with no immunity (i.e. unvaccinated and no prior infection); $t_{LOS,i}$ is the average length of hospital stay estimated from MOH data on duration of patients receiving hospital treatment for Covid-19; $\mu_i$ is the all-cause death rate per 1000 people per year. The age-dependence in $IHR_i$ and $IFR_i$ is based on the results of Herrera-Esposito and de Los Campos (2022) but are scaled down for consistency with New Zealand's observed hospitalisation and death rates, reflecting a combination of the virulence of Omicron relative to earlier variants and tightening definitions to exclude incidental hospitalisations and deaths. The values of $IHR_i$ the Table are multiplied by a factor $\alpha_{IFR} \sim U(0.5, 1.5)$ and the values of $IHR_i$ are multiplied by a factor $\alpha_{IHR} \sim U(0.5, 1.5)$. Total birth rate $b = 59637$ yr$^{-1}$.

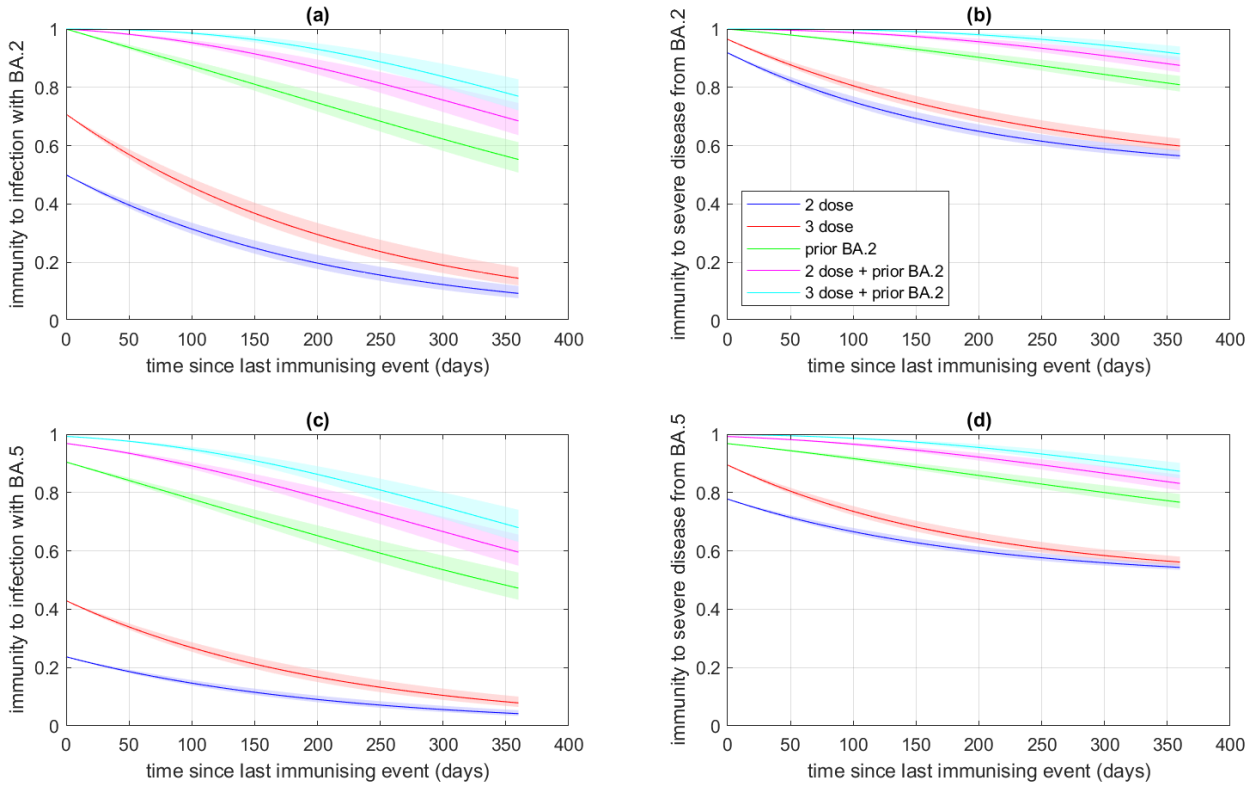


Figure 6: Average immunity against: (a) infection with BA.2; (b) severe disease or death from BA.2; (c) infection with BA.5; (d) severe disease or death from BA.5 as a function of time since most recent immunising event. Graphs show immunity following 2 doses (blue), 3 doses (red), 0/1 doses and prior infection with BA.2 (yellow), 2 doses and prior infection with BA.2 (purple) and 3 doses and prior infection with BA.2 (green).Immunity from two or more prior infections also follows the green trajectory, regardless of vaccination status. Immunity against BA.5 derived from prior infection with BA.5 is assumed to follow the same curves as for immunity against BA.2 derived from prior infection with BA.2. Curves are the median and shaded areas are the interquartile range of 500 model simulations.

with the resident variant), but people infected after $t = t_{VOC}$ (assumed to be infection with the new variant) start with the same initial antibody titre as before the new variant arrived. Thus the model has an equally high level of homologous immunity against reinfection with the same variant (whether resident→resident or VOC→VOC) but a relatively lower level of cross-reactive immunity to the new variant (resident→VOC).

This is implemented in the ODE model with a time-limited increase in the waning fluxes in Eq. (19) for the post-infection compartments:

$$W_{ik} = \left(r_w + r_{VOC}\phi\left(\frac{t - t_{VOC}}{\sigma_{VOC}}\right)\right)\left(\sum_{l=1}^{n_S} S_{il}Q_{lk}^S + \hat{r}\sum_{l=1}^{n_S} R_{il}Q_{lk}^R\right), \qquad k = 11, 12, 13, 14 \quad (30)$$

where $\phi(.)$ is the standard normal probability density function. This formulation means that movement of people to a lower post-infection immunity compartment takes place at $t = t_{VOC}$ in a short time window of duration determined by the parameter $\sigma_{VOC}$. In the limit $\sigma_{VOC} \to 0$, this movement occurs as an instantaneous pulse; larger values of $\sigma$ correspond to a more gradual change.

The magnitude of the drop in infection-derived immunity to the new variant is determined by the dimensionless parameter $r_{VOC}$. In practice, the value of $r_{VOC}$ was chosen such that the change in epidemic growth rate at time $t = t_{VOC}$ corresponds to the empirically observed growth advantage of the new variant relative to the resident variant in genome sequencing data . Similarly, the time $t_{VOC}$ at which the new variant becomes dominant was estimated by extrapolating the empirically observed exponential trend in the ratio of the new variant to resident variant. This simplified approach has provided good estimates to date of the relative growth dynamics of resident and new variants internationally and in New Zealand.

The growth rate of BA.5 relative to BA.2 in genomically sequenced New Zealand community cases reported up to 21 June 2022 (ESR, 2022b) was estimated to be $0.10 \pm 0.027$ day$^{-1}$ via multinomial regression (Supp. Fig. 1). This is consistent with international estimates of the growth advantage of BA.5 over BA.2 which are generally in range 0.07 to 0.14 day$^{-1}$ (UKHSA, 2022). Values of $r_{\mathrm{VOC}} = 0.39 \pm 0.2$ were found to produce an increase in epidemic growth rate consistent with these estimates.

## 3.7 Parameter inference and model fitting

We take a simple approximate Bayesian computation (ABC rejection) approach to inference of key parameter values and fitting the model to data. For each combination of parameter values drawn from the prior, we solve the ODE model and calculate the error function $d(x, y)$ where $x$ is the time series of model outputs for a specified variable and $y$ is the corresponding data time series. We fit the following model outputs:

1. New cases per day, $x_{\mathrm{cases},t} = \alpha_2 \sum_i C_{i2}(t)$.
2. Proportion of new cases in over 60s, $x_{>60,t} = \sum_{i\geq 13} C_{i2}(t) / \sum_i C_{i2}(t)$.

3. New admissions per day, $x_{\text{hosp},t} = \alpha_3 \sum_i H_{i3}(t)$.
4. New deaths per day, $x_{\text{deaths},t} = \alpha_5 \sum_i F_{i5}(t)$.
5. New infections per day, $x_{\text{infections},t} = 1/t_E \sum_{i,k} E_{ik}(t)/N_i(t)$.

Outputs (1) and (2) were fitted to data on new daily cases reported from 1 March to 7 July 2022, smoothed using a 7-day rolling average. The start date of 1 March was chosen to avoid using data from a period at the start of the first Omicron wave when case ascertainment was likely significantly lower due to a lack of testing availability.

Output (3) was fitted to new daily hospital admissions from 1 February to 28 May 2022, smoothed using a 7-day rolling average. The chosen end date ignores the most recent 40 days of data to allow for reporting lags. Only hospital admissions categorised by the Ministry of Health as "Covid-related hospitalisation" were included – this is significantly fewer than the totals reported in the daily updates from the Ministry of Health which include all Covid-positive hospital admissions.

Output (4) was fitted to daily deaths 1 February to 27 June 2022, smoothed using a 7-day rolling average. The chosen end date ignores the most recent 10 days of data to allow for reporting lags. Deaths where the cause-of-death summary was recorded as "COVID as underlying" ($n = 639$), "COVID as contributory" ($n = 358$), or "Not available" ($n = 818$) were included; deaths where the cause-of-death summary was "Not COVID" ($n = 349$) were excluded.

Output (5) was fitted to data on the weekly incidence of new cases in a routinely tested cohort of approximately 20,000 border workers from 13 February to 3 July 2022. This may not be a representative sample of the population but we include it because, unlike outputs (1–4), it provides longitudinal surveillance data that is not affected by either case ascertainment levels or disease severity.

For each these time series, the error function is defined as

$$d(x, y) = 1/n \sum_{t=1}^{n} \left(\ln(x_t + \epsilon) - \ln(y_t + \epsilon)\right)^2 \tag{31}$$

This definition means the error function is dimensionless, insensitive to the number of data points available for fitting, and has the symmetry $d(x, y) = d(y, x)$. Here $\epsilon$ is a fixed value that is small relative to typically values of the variable being fitted: we set $\epsilon = 10$ per day for cases, $\epsilon = 0.5$ for hospital occupancy, $\epsilon = 0.01$ per day for deaths, $\epsilon = 5 \times 10^{-5}$ for age distribution of cases, and $\epsilon = 5 \times 10^{-6}$ per day for incidence per capita.

The total error is defined as

$$d_{\text{total}} = w_1 d_{\text{cases}} + w_2 d_{>60} + w_3 d_{\text{hosp}} + w_4 d_{\text{deaths}} + + w_5 d_{\text{infections}} \tag{32}$$

where we used $w_j = 1$ so each time series received equal weighting. We used an ABC rejection algorithm: we solved the model for $N = 50000$ parameter combinations drawn randomly from the prior and retained the 500 simulations with the smallest error.

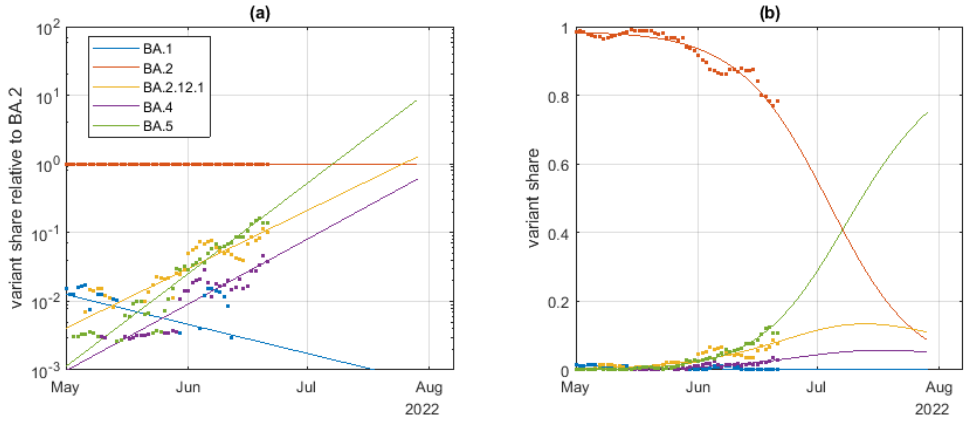


Supplementary Figure 1: Proportion of sequenced community cases reported up to 21 June 2022 that were categorised by ESR (2022b) as BA.1, BA.2, BA.2.12.1, BA.4 and BA.5 (points) together with a multinomial regression model (curves). Panel (a) shows the share of each sub-variant relative to the previously dominant BA.2 sub-variant; (b) shows the absolute share of each sub-variant. The growth rate of BA.5 relative to BA.2 was estimated in the multinomial regression model to be $0.1 \pm 0.027$ day$^{-1}$.

Prior distributions for fitted parameters are shown in Tables 1 and 2. Generally, informative priors were used that represent reasonable uncertainty in parameter estimates. These include changes in the value of the reproduction number excluding immunity $R_{EI}(t)$ and contact matrix $M$ during specified time windows, to model changes in mixing rates as a result of public health interventions or voluntary behavioural change. The value of $R_{EI}(t)$ was assumed to increase linearly from $R_{EI,1}$ to $R_{EI,2}$ starting around 10 March 2022 and over a window of 30–50 days (see Table 2). The contact matrix $M$ was initially set to the matrix in Vattiato et al. (2022), denoted $M_0$, to provide a reasonable match with the observed age distribution of cases in the first part of the simulated time period. The contact matrix $M$ was assumed to change to a modified matrix $(1 - \alpha_M)M_0 + \alpha_M M_1$, where $M_1$ is the matrix estimated from pre-pandemic data (Prem et al., 2017; Steyn et al., 2022) and $\alpha_M \in [0, 1]$ is fitted to data. The change in contact matrix was assumed to occur linearly over a 70–90 day time windows starting at the same time as the change in $R_{EI}(t)$ (see Table 2). These are ad hoc model adjustments that were observed to provide a reasonable fit to data and reflect plausible behavioural changes during the simulated time period.

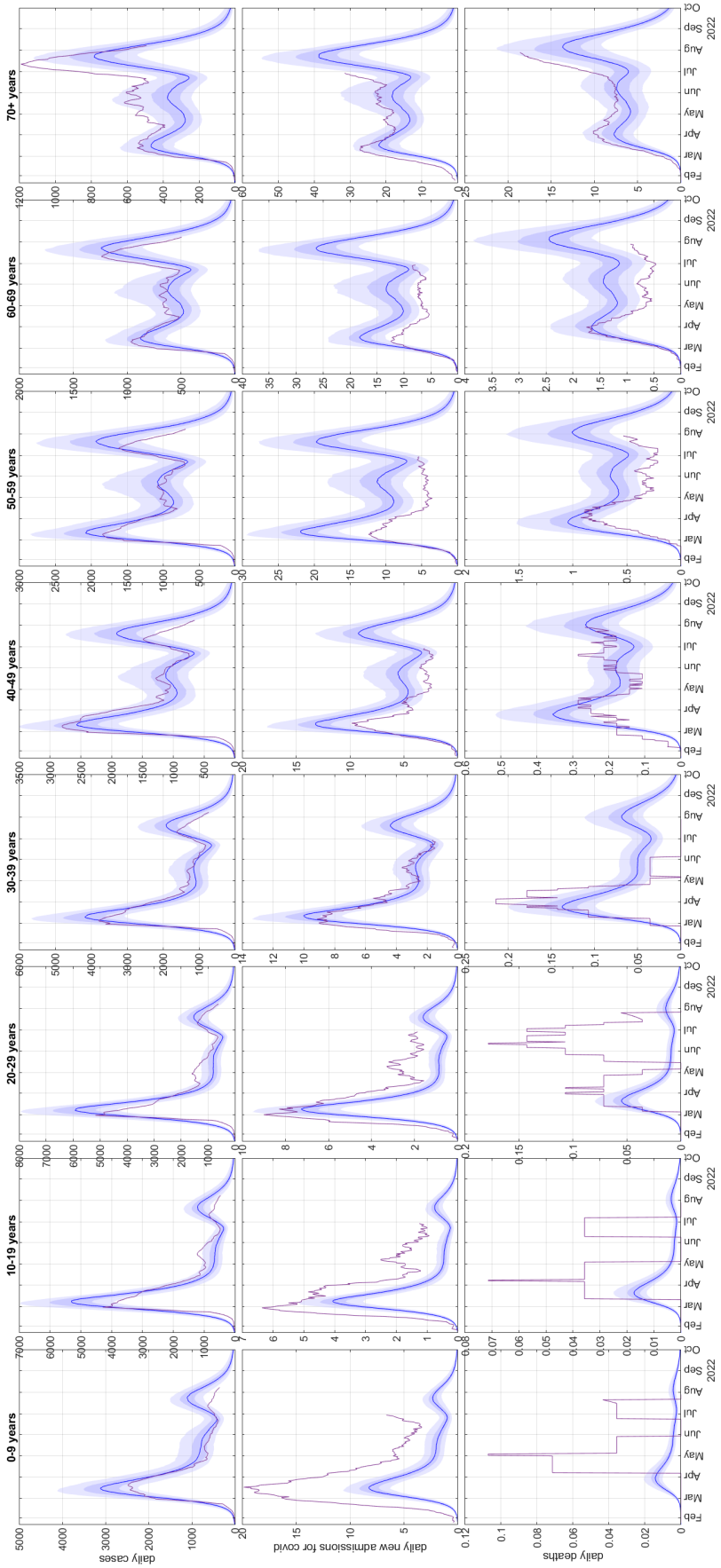


Supplementary Figure 2: Age-stratified results for the baseline scenario showing new daily cases, new daily hospital admissions and daily deaths. Blue curve shows the median of 500 model simulations and shaded bands show the 5th, 25th, 75th and 95th percentiles. Data (purple curves) is shown as a rolling average over 7 days for cases, 14 days for admissions and 28 days for deaths.

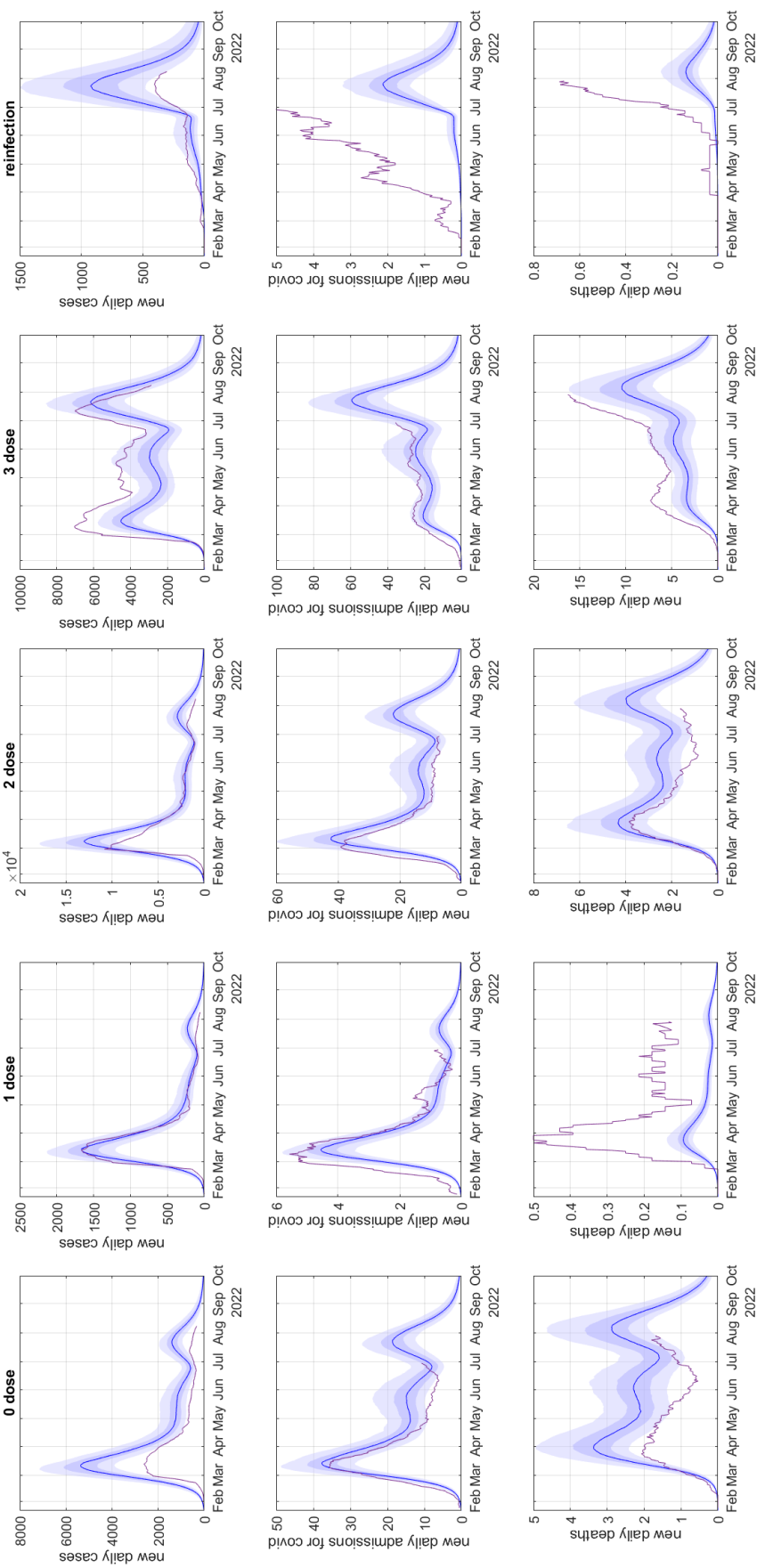


Supplementary Figure 3: Results stratified by immunity status (no prior infections and 0 doses, no prior infections and 1 dose, no prior infections and 2 doses, no prior infection and at least 3 doses, and with prior infection) for the baseline scenario showing new daily cases, new daily hospital admissions and daily deaths. Data on reinfections show individuals with a positive test result reported at least 28 days after a previous positive test results; this definition may include some chronic infections. Model results for reinfecitons are adjusted for under-ascertainment of the first infection according to the age-specific case ascertainment ratio in the model. Note this assumes that reporting of first infection and subsequent reinfections occur with independently with the same probability, so the comparison should be viewed as approximate. Blue curve shows the median of 500 model simulations and shaded bands show the 5th, 25th, 75th and 95th percentiles. Data (purple curves) show the rolling average over 7 days for cases, 14 days for admissions and 28 days for deaths.

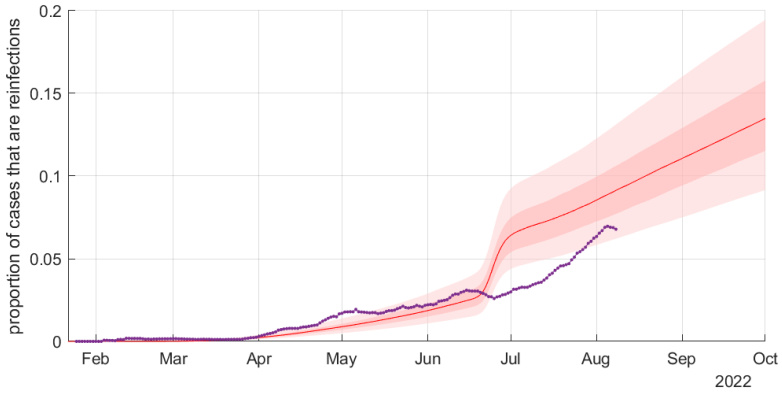


Supplementary Figure 4: Proportion of new reported cases that are reinfections. Model results (red curve and bands) show the proportion of new reported cases that are reinfections, adjusted for under-ascertainment of the first infection according to the age-specific case ascertainment ratio in the model. Note this assumes that reporting of first infection and subsequent reinfections occur with independently with the same probability, so the comparison should be viewed as approximate. Red curve shows the median of 500 model simulations and shaded bands show the 5th, 25th, 75th and 95th percentiles. Data (purple points) show the 7-day rolling average number of new cases that have previously reported a positive SARS-CoV-2 test at least 28 days previously as a fraction of the 7-day rolling average of total new cases.

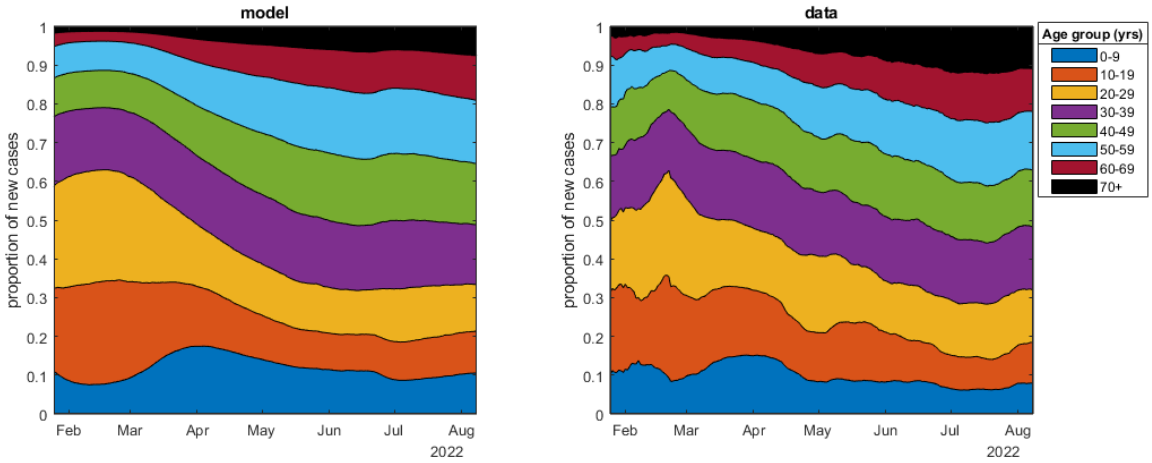


Supplementary Figure 5: Age distribution of new cases in the model compared to the data, shown as the 7-day rolling average.

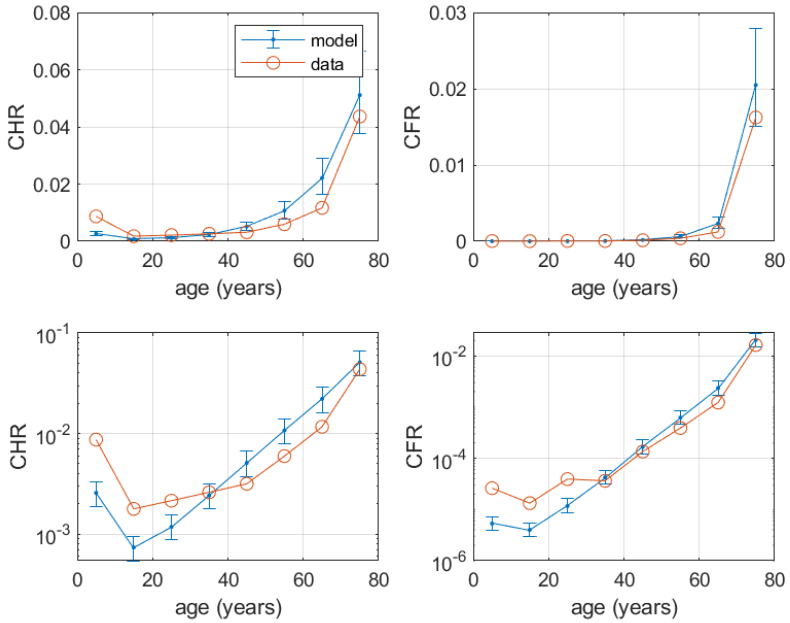


Supplementary Figure 6: Age-specific case hospitalisation ratio (CHR) and case fatality ratio (CFR). Upper plots show results on a linear scale; lower plots show results on a log scale.

## Acknowledgements

The authors acknowledge the role of the New Zealand Ministry of Health, StatsNZ, and the Institute of Environmental Science and Research in supplying data in support of this work. The authors are grateful to Michael Bunce, Emily Harvey, August Hao, Nick Golding, James McCaw, Dion O'Neale, Gerry Ryan, Freya Shearer and David Welch for discussions about modelling immunity and the growth of BA.5, and to Nigel French, Markus Luczak-Roesch, Matt Parry, and the Covid-19 Modelling Government Steering Group for feedback on earlier versions of this report. This work was funded by the New Zealand Department of Prime Minister and Cabinet.

# References

Altarawneh, H. N., Chemaitelly, H., Ayoub, H., Hasan, M. R., Coyle, P., YASSINE, H. M., Al Khatib, H. A., Benslimane, F., Al-Kanaani, Z., Al Kuwari, E., et al. (2022). Protection of SARS-CoV-2 natural infection against reinfection with the BA.4 or BA.5 Omicron subvariants. *medRxiv*, https://doi.org/10.1101/2022.07.11.22277448.

Cao, Y., Yisimayi, A., Jian, F., Song, W., Xiao, T., Wang, L., Du, S., Wang, J., Li, Q., Chen, X., et al. (2022). BA.2.12. 1, BA.4 and BA.5 escape antibodies elicited by Omicron infection. *Nature*, https://doi.org/10.1038/s41586-022-04980-y.

Cromer, D., Steain, M., Reynaldi, A., Schlub, T. E., Sasson, S. C., Kent, S. J., Khoury, D. S., and Davenport, M. P. (2022a). Neutralising antibodies predict protection from severe COVID-19. *medRxiv*, https://doi.org/10.1101/2022.06.09.22275942.

Cromer, D., Steain, M., Reynaldi, A., Schlub, T. E., Wheatley, A. K., Juno, J. A., Kent, S. J., Triccas, J. A., Khoury, D. S., and Davenport, M. P. (2022b). Neutralising antibody titres as predictors of protection against sars-cov-2 variants and the impact of boosting: a meta-analysis. *Lancet Microbe*, 3(1):e52–e61.

ESR (2022a). Genomics insights dashboard. https://esr2.cwp.govt.nz/our-expertise/covid-19-response/covid19-insights/genomics-insights-dashboard/. Accessed 2 July 2022.

ESR (2022b). Prevelence of SARS-CoV-2 variants of concern in Aoteoroa New Zealand. https://github.com/ESR-NZ/nz-sars-cov2-variants.

Golding, N. and Lydeamore, M. (2022). Analyses to predict the efficacy and waning of vaccines and previous infection against transmission and clinical outcomes of SARS-CoV-2 variants. https://github.com/goldingn/neuts2efficacy. Accessed 5 April 2022.

Hachmann, N. P., Miller, J., Collier, A.-r. Y., Ventura, J. D., Yu, J., Rowe, M., Bondzie, E. A., Powers, O., Surve, N., Hall, K., et al. (2022). Neutralization escape by SARS-CoV-2 Omicron subvariants BA.2.12.1, BA.4, and BA.5. *New England Journal of Medicine*, 387:86–88.

Hansen, C. H., Friis, N. U., Bager, P., Stegger, M., Fonager, J., Fomsgaard, A., Gram, M. A., Engbo Christiansen, L., Ethelberg, S., Legarth, R., et al. (2022). Risk of reinfection, vaccine protection, and severity of infection with the BA.5 Omicron subvariant: A Danish nationwide population-based study. *Available at SSRN*, https://dx.doi.org/10.2139/ssrn.4165630.

Herrera-Esposito, D. and de Los Campos, G. (2022). Age-specific rate of severe and critical sars-cov-2 infections estimated with multi-country seroprevalence studies. *BMC Infectious Diseases*, 22(1):1–14.

Keeling, M. J., Brooks-Pollock, E., Challen, R. J., Danon, L., Dyson, L., Gog, J. R., Guzman-Rincon, L., Hill, E. M., Pellis, L. M., Read, J. M., et al. (2021). Short-term projections based on early omicron variant dynamics in england. *medRxiv*, https://doi.org/10.1101/2021.12.30.21268307.

Khan, K., Karim, F., Ganga, Y., Bernstein, M., Jule, Z., Reedoy, K., Cele, S., Lustig, G., Amoako, D., Wolter, N., et al. (2022). Omicron sub-lineages BA.4/BA.5 escape BA.1 infection elicited neutralizing immunity. *medRxiv*, https://doi.org/10.1101/2022.04.29.22274477.

Khoury, D. S., Cromer, D., Reynaldi, A., Schlub, T. E., Wheatley, A. K., Juno, J. A., Subbarao, K., Kent, S. J., Triccas, J. A., and Davenport, M. P. (2021). Neutralizing antibody levels are highly predictive of immune protection from symptomatic sars-cov-2 infection. *Nature Medicine*, 27(7):1205–1211.

Malato, J., Ribeiro, R. M., Leite, P. P., Casaca, P., Fernandes, E., Antunes, C., Fonseca, V. R., Gomes, M. C., and Graca, L. (2022). Risk of BA.5 infection in individuals exposed to prior SARS-CoV-2 variants. *medRxiv*, https://doi.org/10.1101/2022.07.27.22277602.

Ministry of Health (2022). New Zealand COVID-19 data. https://github.com/minhealthnz/nz-covid-data/tree/main/cases.

Prem, K., Cook, A. R., and Jit, M. (2017). Projecting social contact matrices in 152 countries using contact surveys and demographic data. *PLoS Computational Biology*, 13(9):e1005697.

StatsNZ (2022). Infoshare. https://infoshare.stats.govt.nz. Accessed 29 May 2022.

Steyn, N., Binny, R. N., Hannah, K., Hendy, S., James, A., Lustig, A., Ridings, K., Plank, M. J., and Sporle, A. (2021). Māori and Pacific people in New Zealand have higher risk of hospitalisation for COVID-19. *New Zealand Medical Journal*, 134:28–43.

Steyn, N., Plank, M. J., Binny, R. N., Hendy, S. C., Lustig, A., and Ridings, K. (2022). A COVID-19 vaccination model for Aotearoa New Zealand. *Scientific Reports*, 12(1):1–11.

Tegally, H., Moir, M., Everatt, J., Giovanetti, M., Scheepers, C., Wilkinson, E., Subramoney, K., Makatini, Z., Moyo, S., Amoako, D. G., et al. (2022). Emergence of SARS-CoV-2 Omicron lineages BA.4 and BA.5 in South Africa. *Nature Medicine*, https://doi.org/10.1038/s41591-022-01911-2.

Tuekprakhon, A., Huo, J., Nutalai, R., Dijokaite-Guraliuc, A., Zhou, D., Ginn, H. M., Selvaraj, M., Liu, C., Mentzer, A. J., Supasa, P., et al. (2022). Antibody escape of SARS-CoV-2 Omicron BA.4 and BA.5 from vaccine and BA.1 serum. *Cell*, 185:2422–2433.e13.

UKHSA (2022). SARS-CoV-2 variants of concern and variants under investigation in England. Technical briefing 42. https://www.gov.uk/government/publications/investigation-of-sars-cov-2-variants-technical-briefings.

Vattiato, G., Maclaren, O., Lustig, A., Binny, R. N., Hendy, S. C., and Plank, M. J. (2022). An assessment of the potential impact of the Omicron variant of SARS-CoV-2 in Aotearoa New Zealand. *Infectious Disease Modelling*, 7:94–105.